Polychromatic Cherenkov Radiation Induced Group Velocity Symmetry Breaking in Counterpropagating Dissipative Kerr Solitons

Wenle Weng, Romain Bouchand, Erwan Lucas, and Tobias J. Kippenberg

Phys. Rev. Lett. **123**, 253902 — Published 17 December 2019

DOI: 10.1103/PhysRevLett.123.253902

Polychromatic Cherenkov radiation induced group velocity symmetry breaking in counterpropagating dissipative Kerr solitons

Wenle Weng,* Romain Bouchand, Erwan Lucas, and Tobias J. Kippenberg†
Institute of Physics, École Polytechnique Fédérale de Lausanne (EPFL), CH-1015 Lausanne, Switzerland

High-order-dispersion-induced dispersive waves emitted by dissipative Kerr solitons are frequently observed in microresonator frequency comb generation. Also known as soliton Cherenkov radiation, this type of dispersive wave plays a critical role in comb spectrum broadening as well as formation of soliton bound states. Here, we report the experimental observation of symmetry breaking in the group velocity of counterpropagating solitons in a crystalline microresonator. Induced by the polychromatic Cherenkov radiation, soliton bound states are formed, showing different group velocities with different spatiotemporal separations between constituent solitons. By bidirectionally pumping the microresonator with laser fields of equal power and frequency, we demonstrate the degeneracy lifting of repetition rates of the counterpropagating solitons. Our work not only shines new light on the impact of dispersive waves in nonlinear cavities, but also introduces a novel approach to develop compact dual-comb spectrometers.

Dispersive waves are of importance in the study of wave propagation in hydraulics [1], solid mechanics [2], magnetic systems [3] and ecology [4]. In optics, dispersive wave formation [5] has played a pivotal role in the development of self-referenced frequency combs [6, 7] by enabling coherent octave spanning spectra via supercontinuum [8–11]. Analogous to classical Cherenkov radiation (CR) that occurs when a charged particle passes through a dielectric medium at a speed exceeding the phase velocity of light, dispersive waves can be emitted by dissipative cavity solitons when the soliton phase velocity matches that of a spectrally separated wave, leading to oscillatory tails at the trailing or leading edge of the solitons [12–15]. In recent years, the generation of CR with dissipative Kerr solitons (DKS) has given rise to broadband and coherent microresonator frequency combs (microcomb) [16]. In this context, CR has been utilized for achieving comb self-referencing [17], octave spanning of comb spectrum [18], microcomb stabilization [19], and deterministic single-soliton microcomb inception [20]. In addition, CR can be used as a means of tuning the soliton group velocity and consequently the microcomb repetition rate [13, 14, 21–24], which on the one hand may facilitate the agile control of comb line spacing, but on the other hand constitutes a noise transduction mechanism for microwave generation based on Kerr microresonators [22, 25].

In this work, we demonstrate that soliton CR can lead to the symmetry breaking of the repetition rate of counterpropagating (CP) DKS. In contrast to earlier works that deliberately imposed an asymmetry in either pump power [26] or laser frequency [27], we observe that, even with pumping fields of identical power, polarization and frequency, CP DKS can have distinct group velocities. As conceptually illustrated by Fig. 1, under symmetric pumping conditions, the CP DKS group velocity symmetry can be broken if (1) the clockwise (CW) and the counter-clockwise (CCW) states are of unequal soliton numbers; or (2) the CW and the CCW states are of multi-soliton states with equal soliton numbers but dissimilar spatiotemporal arrangements. Such microcomb repetition rate symmetry breaking mechanism constitutes a simple yet powerful method to perform dual-comb spectroscopy using a single laser, and within a single whispering gallery mode (WGM) family. To offer insight into this phenomenon, we simulate the soliton bound states in a Kerr cavity with high-order dispersions. We reveal that the polychromatic CR induced by individual solitons can interact with co-propagating solitons and their corresponding CR. Such interaction forms multi-soliton bound states, and induces DKS group velocity variations with different inter-soliton separations due to the soliton recoil effect [5, 13, 28].

Fig. 2 (a) illustrates the experimental setup. A configuration of CP solitons in a single WGM family in a crystalline MgF_2 resonator is ultilized due to the perfect symmetric pump condition it allows. The resonator has a free spectral range (FSR) of 14.09 GHz. A tapered fiber is used to evanescently couple light into and out of the resonator, with a loaded quality factor (Q) of $\sim 1 \times 10^9$.

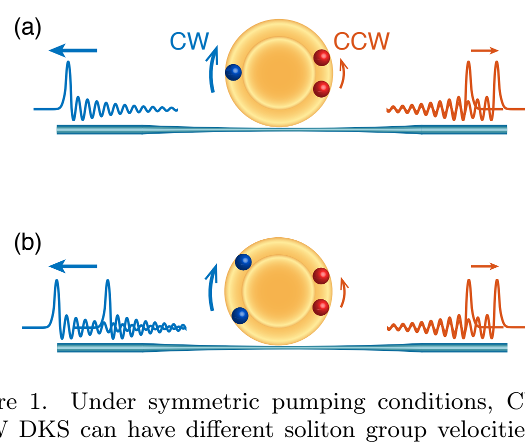

Figure 1. Under symmetric pumping conditions, CW and CCW DKS can have different soliton group velocities if (a) the CP states are of unequal soliton numbers; or (b) the CP states are multi-soliton states with equal soliton numbers but unequal inter-soliton separations.

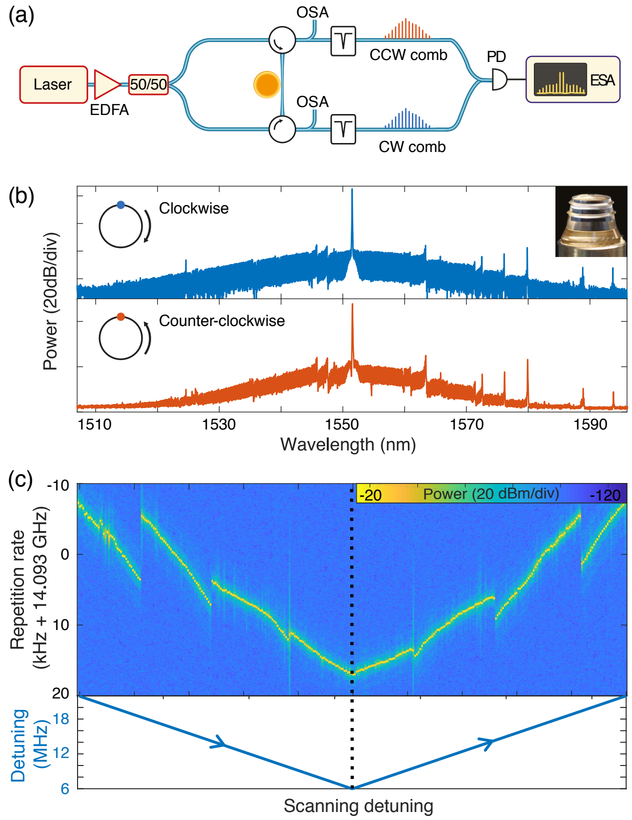

Figure 2. (a) Experimental setup. (b) Optical spectra of the single-soliton states in the CW (blue) and CCW (red) directions. A picture of the microresonator is shown in the inset. (c) Soliton repetition rate spectrogram obtained from the combination of two CP soliton states while scanning the detuning over 16 MHz. The step size of the scanning is 100 kHz. At each step, after the detuning is changed, stable microcomb optical spectra and repetition rate spectrum are acquired.

A 1550-nm laser is amplified by an erbium-doped fiber amplifier (EDFA) to 400 mW. A 50/50 splitter and two fiber circulators are used to pump a single spatial mode with CW and CCW fields of equal intensities. By downsweeping the laser frequency over the mode resonances we are able to generate CW and CCW DKS, whose microcomb spectra and repetition rates are monitored by two optical spectrum analyzers (OSAs) and an electrical spectrum analyzer (ESA). When both directions are of single-soliton state (see Fig. 2 (b) for the single-soliton comb spectra), the repetition rates of both microcombs shown in Fig. 2 (c) remain degenerate as the detuning is tuned over 16 MHz, despite several discontinuities that are attributed to the bistability induced by single-mode dispersive waves [22, 29]. Due to the large number of spatial modes the resonator can hold, the microcomb spectra exhibit a number of pronounced CR emissions at various wavelengths due to mode crossings caused by spatial mode interactions [28, 30, 31]. By monitoring the microcomb spectra we find that these CR emissions in the CW microcomb behave the same as those in the CCW microcomb, i. e. showing almost identical relative intensities and becoming stronger or weaker at the same time. Such observations clearly show that the CW and CCW microcomb states are dynamically symmetrical. One should note that even with a small level of inequality in the bidirectional pumping intensities and frequencies, CP DKS can still maintain the repetition rate degeneracy due to the interlocking effect that is caused by the back-scattering [27]. Our separate measurement shows that the interlocking can be sustained until the repetition rate difference surpasses a few hundred Hz (see Supplemental Material [32] for details).

Next, with DKS number switching technique [33], we generate a CW single-soliton state and a CCW dual-soliton state whose comb spectra are presented in Fig. 3 (a). It is well known that CR of a soliton can interact with other solitons, forming soliton bound states via dispersive-wave-mediated soliton interactions [34–36]. On the one hand, the CR manifests as a modulation of the intracavity field background that is bound to the soliton [5] and which provides a trapping potential for multi-soliton states [37]. On the other hand, the CR constitutes a loss mechanism where energy is radiated from the solitons and induces a shift of the soliton group velocity in a deterministic way (spectral recoil effect). Moreover, because CR in practical settings are normally broadband (induced by third-order dispersion) or polychromatic (induced by multiple spatial mode interactions), the interference between CR of multiple solitons can be very complex, and certain CR emissions can be either enhanced or suppressed by the interference. Compounded by the CR-induced detuning bistability [22, 29], it is reasonable to expect a multi-soliton DKS to have a soliton group velocity that is different from that of a single-soliton state due to the different recoil strengths at certain detunings. Indeed, as shown in Fig. 3 (b), we observe that the CP DKS feature non-degenerate group velocities (i. e. the CW DKS repetition rate $f_{\mathrm{rep}}^{\mathrm{cw}}$ is different from the CCW DKS repetition rate $f_{\mathrm{rep}}^{\mathrm{ccw}}$) at several detuning regions as we scan the pump-resonance detuning over 10 MHz. In these regions two prominent repetition rate signals as well as multiple weak modulational signals are detected, with a splitting of the repetition frequency that is typically of a few kHz. In addition, in stark contrast to the situation where both CW and CCW are of single-soliton state, the polychromatic CR in the single-soliton state and the dual-soliton state exhibit different behaviors. As an example, in Fig. 3 (c) we plot the optical intensity of a mode that is separated from the pumped mode by 246 FSRs. We denote the mode order number as $\mu = 246$ while the pumped mode is of $\mu = 0$. Strong CR amplitudes are found in this mode, as presented in Fig. 3 (a). This mode also shows notable bistability with different detuning scanning directions, and the bistability occurs at different detuning regions for CW and CCW

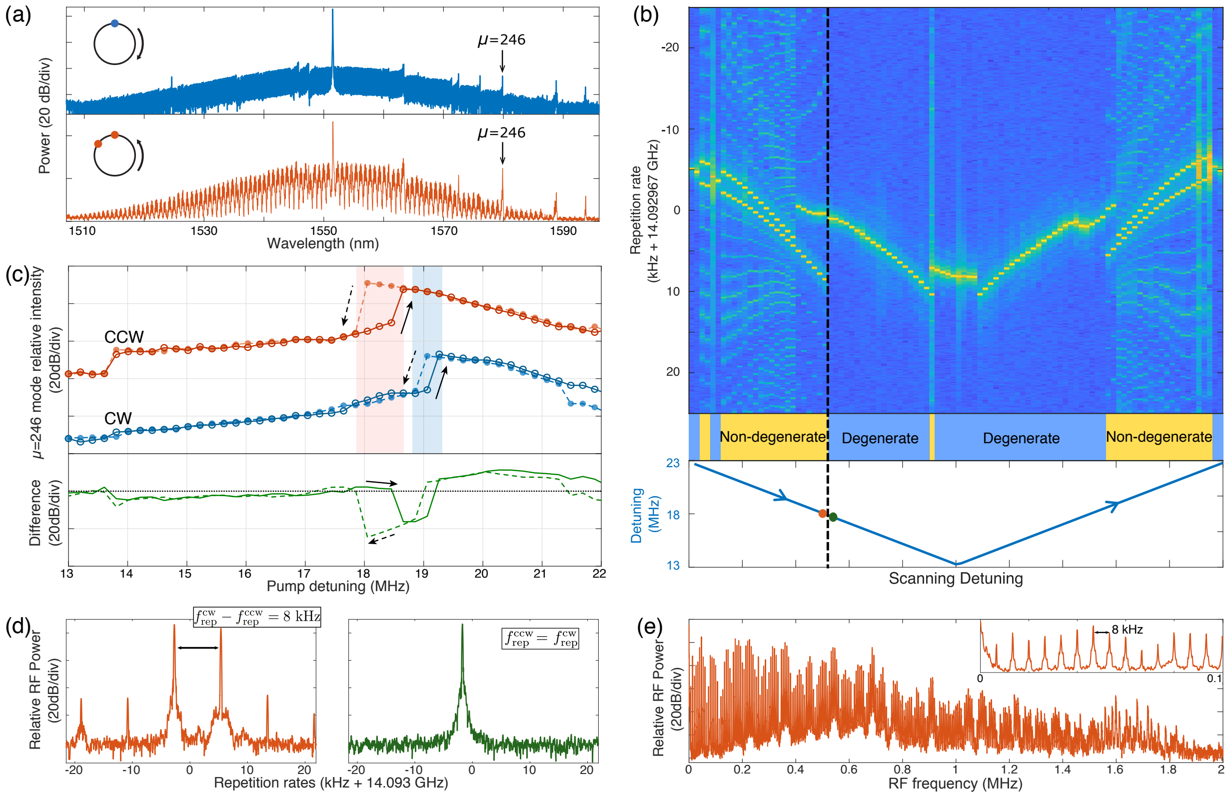

Figure 3. (a) Microcomb spectra of a CW single-soliton state (blue) and a CCW dual-soliton state (red). (b) Evolution of the CP DKS repetition rates when the pump-resonance detuning is scanned. In the regions where the degeneracy is lifted (indicated by the lower yellow strips), the higher (lower) repetition rate corresponds to the CW (CCW) DKS because the signal shows slightly higher (lower) amplitude. Around the two prominent repetition rate signals we observe multiple modulation sidebands, which we attribute to the collision between CW and CCW solitons in the microresonator. (c) The upper figure shows the relative CR intensities in a mode (order number $\mu = 246$) in the CW (blue) and the CCW (red) microcombs. Strong bistabilities with increasing detuning (open circles and solid lines) and decreasing detuning (shallow circles with dashed lines) are indicated by the shaded areas. The lower figure plots the relative intensity difference with different detuning sweeping directions. The black dotted line indicates the equal relative intensities. (d) The non-degenerate (left) and the degenerate (right) repetition rate spectra that correspond to the red and green dots shown in the lower panel in (b). The resolution bandwidth (RBW) is 500 Hz. (e) The RF comb obtained when the repetition rate degeneracy is lifted. The line spacing of the RF comb is equal to the frequency difference between the repetition rates of the CW and CCW solitons. The inset shows a portion of the comb in the frequency range of 0 – 0.1 MHz.

solitons. Consequently, the CR amplitudes in CW and CCW directions are significantly different in regions that are shaded in colors, which in turn, cause different recoil impact on the DKS and shift DKS group velocities as well as the carrier frequencies of solitons and CR by different amounts. Since the microcombs in this study show observable CR in many modes across the comb spectra, to accurately quantify the combined effect of all CR emissions is non-trivial and beyond the scope of this work. In [32] we adopt simplified models to simulate the DKS group velocity shifts under the influence of polychromatic CR. The simulation results are in qualitative agreement with the experimental observations.

The lifting of the group velocity degeneracy offers a straigtforward approach to generate a dual-comb spectrum [38] at low frequency ranges. In Fig. 3 (e) the radio-frequency (RF) spectrum generated by the beating of the two combs is presented. The pump-resonance detuning is set to be 18 MHz. The dual-comb configuration is corroborated by the baseband structure observed on the ESA. It consists of equidistant RF signals starting from DC as the two microcombs share the same pump laser. The line-spacing of the RF comb is determined by the difference between CW and CCW soliton group velocities. Owing to the relatively small repetition rate difference ($\Delta f_{\rm rep}$) and the fact that the RF comb starts at DC, the dual-comb system strongly relaxes the photodetection bandwidth requirement, and leads to a large optical-to-RF mapping factor of approximately 10^6.

In order to reveal the dual-soliton repetition rate's dependence on the inter-soliton separation, we experimentally compare the repetition rates of CP dual-soliton states that are of identical or distinct inter-soliton separations. First, in both directions we generate dual-

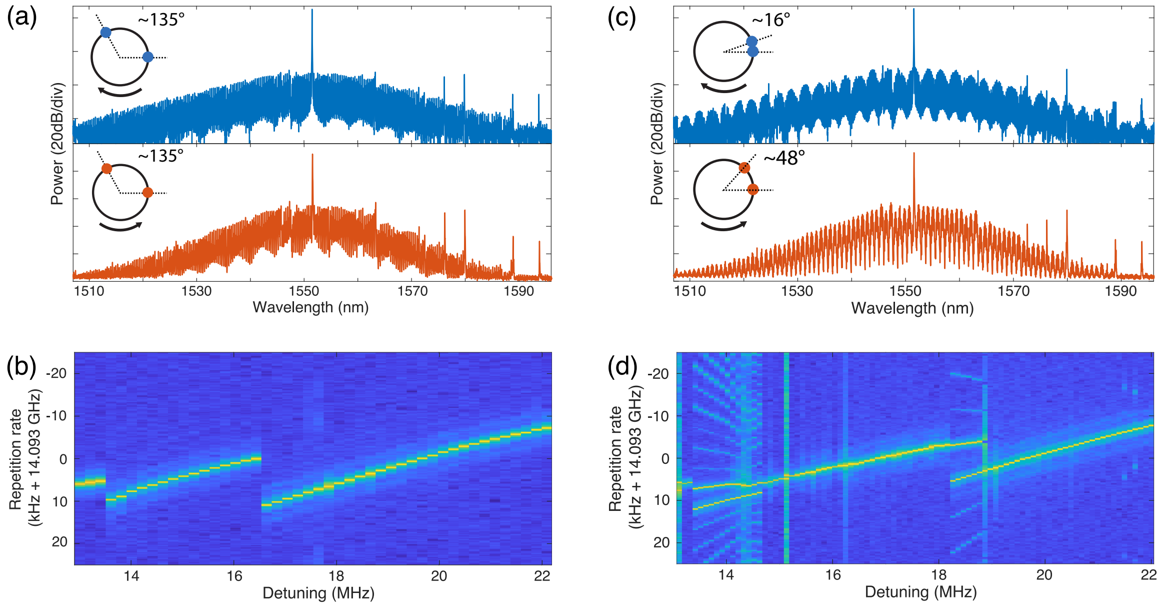

Figure 4. (a) Comb spectra of the dual-soliton states in the CW (blue) and CCW (red) directions, showing identical inter-soliton separations. The insets display the estimated temporal separations in the dual-soliton states. (b) Soliton repetition rate spectrogram of the identical CP DKS, showing a single repetition rate signal the whole time. (c) Comb spectra of the CW and CCW dual-soliton states that are of different temporal arrangements. (d) The repetition rate spectrogram of the dissimilar dual-soliton states exhibit several regimes where degeneracy is lifted.

soliton states that are of exactly same temporal arrangement (see [32] for details of the generation approach). In Fig. 4 (a) are the comb spectra of the CW and CCW DKS. Several strong single-mode dispersive waves are observed at the same locations in both spectra. Only one repetition rate is observed as the pump-resonance detuning is scanned over ~ 10 MHz (Fig. 4 (b)), suggesting that the symmetry is preserved the whole time. We then repeat the detuning scanning experiment with CP dual-soliton states that obviously have dissimilar inter-soliton separations. The corresponding microcomb spectra are presented in Fig. 4 (c). This time we observe noticeable difference in the CR spectra in the two combs. Remarkably, as displayed in Fig. 4 (d), in several detuning regions the CP DKS exhibit double repetition rates, showing symmetry breaking in soliton group velocity.

Here we discuss the significance of this work. Previous studies [34–36] on dispersive waves' role in the formation of DKS bound states, mostly based on theoretical and numerical analysis, have already implied that DKS bound states would have different group velocities if their structures are different. Our work takes advantage of the large number of mode crossings in a WGM resonator to demonstrate the DKS group velocity variation with mode-crossing-induced polychromatic CR. It corroborates earlier studies with convincing experimental results. It is of particular importance to mention that a mode-crossing-induced CR often can be approximated by a single-mode CR [22], which effectively enhances only one comb tooth, and creates a quasi-periodic intracavity potential traps. Such quasi-periodic traps lead to multi-DKS bound states with constructive CR interference [20], hence the CR intensity is quadratically proportional to the number of DKS. As a result, the DKS group velocity is almost unaffected by the inter-soliton separations as long as the soliton number in the bound state remains the same. Conversely, as shown by our experiments, interference of polychromatic CR is complicated and may significantly vary the DKS group velocity with different choices of bound state structure. The complex nature of the soliton binding also can be related to the case of 2D soliton bound states [39].

For practical applications, our work demonstrates a simple dual-comb generation scheme by turning the usually undesired multiple mode crossings into an advantage in manipulation of microcomb repetition frequency. Admittedly, the generated RF comb spectrum is not as smooth as those generated by two single-soliton microcombs, and the use of one pumping laser results in folding of the RF comb [27, 40], which would reduce the usable spectral range in dual-comb spectroscopy applications. Yet, with extra filtering [40] or a referenced arm [41] these shortcomings can be alleviated. Furthermore, our technique may be applied in microcomb-based lidar system [42, 43] or Vernier spectrometer [44] where it could simplify the system without degrading the coherence.

The code and data used to produce the plots within this Letter are available by following the link in Ref. [46].

The authors thank Connor Skehan for proof-reading the manuscript. This publication was supported by

Contract D18AC00032 (DRINQS) from the Defense Advanced Research Projects Agency (DARPA), Defense Sciences Office (DSO) and funding from the Swiss National Science Foundation under grant agreement No. 165933. W. W. acknowledges support by funding from the European Union's H2020 research and innovation programme under grant agreement No. 753749 (SOLISYNTH).

W. W. and R. B. contributed equally to this work.

* wenle.weng@epfl.ch
† tobias.kippenberg@epfl.ch

[1] G. Whitham, Journal of Fluid Mechanics **22**, 273 (1965).
[2] W. Sachse and Y.-H. Pao, Journal of Applied Physics **49**, 4320 (1978).
[3] B. N. Rogers, R. E. Denton, J. F. Drake, and M. A. Shay, Physical Review Letters **87**, 195004 (2001).
[4] J. Frantzen and F. Van den Bosch, Basic and Applied Ecology **1**, 83 (2000).
[5] N. Akhmediev and M. Karlsson, Physical Review A **51**, 2602 (1995).
[6] T. Udem, R. Holzwarth, and T. W. Hänsch, Nature **416**, 233 (2002).
[7] T. W. Hänsch, Reviews of Modern Physics **78**, 1297 (2006).
[8] J. K. Ranka, R. S. Windeler, and A. J. Stentz, Optics letters **25**, 25 (2000).
[9] J. M. Dudley, G. Genty, and S. Coen, Reviews of Modern Physics **78**, 1135 (2006).
[10] D. V. Skryabin and A. V. Gorbach, Reviews of Modern Physics **82**, 1287 (2010).
[11] C. Markos, J. C. Travers, A. Abdolvand, B. J. Eggleton, and O. Bang, Reviews of Modern Physics **89**, 045003 (2017).
[12] S. Coen, H. G. Randle, T. Sylvestre, and M. Erkintalo, Optics Letters **38**, 37 (2013).
[13] C. Milián and D. Skryabin, Optics Express **22**, 3732 (2014).
[14] J. K. Jang, M. Erkintalo, S. G. Murdoch, and S. Coen, Optics Letters **39**, 5503 (2014).
[15] V. Brasch, M. Geiselmann, T. Herr, G. Lihachev, M. H. P. Pfeiffer, M. L. Gorodetsky, and T. J. Kippenberg, Science **351**, 357 (2016).
[16] T. J. Kippenberg, A. L. Gaeta, M. Lipson, and M. L. Gorodetsky, Science **361**, eaan8083 (2018).
[17] V. Brasch, E. Lucas, J. D. Jost, M. Geiselmann, and T. J. Kippenberg, Light: Science and Applications **6** (2017).
[18] D. T. Spencer, T. Drake, T. C. Briles, J. Stone, L. C. Sinclair, C. Fredrick, Q. Li, D. Westly, B. R. Ilic, A. Bluestone, *et al.*, Nature **557**, 81 (2018).
[19] P. Parra-Rivas, D. Gomila, F. Leo, S. Coen, and L. Gelens, Optics Letters **39**, 2971 (2014).
[20] C. Bao, Y. Xuan, D. E. Leaird, S. Wabnitz, M. Qi, and A. M. Weiner, Optica **4**, 1011 (2017).
[21] E. Lucas, H. Guo, J. D. Jost, M. Karpov, and T. J. Kippenberg, Physical Review A **95**, 043822 (2017).
[22] X. Yi, Q.-F. Yang, X. Zhang, K. Y. Yang, X. Li, and K. Vahala, Nature Communications **8**, 14869 (2017).
[23] A. V. Cherenkov, V. E. Lobanov, and M. L. Gorodetsky, Physical Review A **95**, 033810 (2017).
[24] D. Skryabin and Y. Kartashov, Optics Express **25**, 27442 (2017).
[25] J. Liu, E. Lucas, A. S. Raja, J. He, J. Riemensberger, R. N. Wang, M. Karpov, H. Guo, R. Bouchand, and T. J. Kippenberg, arXiv preprint arXiv:1901.10372 (2019).
[26] C. Joshi, A. Klenner, Y. Okawachi, M. Yu, K. Luke, X. Ji, M. Lipson, and A. L. Gaeta, Optics Letters **43**, 547 (2018).
[27] Q.-F. Yang, X. Yi, K. Y. Yang, and K. Vahala, Nature Photonics **11**, 560 (2017).
[28] A. B. Matsko, W. Liang, A. A. Savchenkov, D. Eliyahu, and L. Maleki, Optics Letters **41**, 2907 (2016).
[29] W. Weng, E. Lucas, G. Lihachev, V. E. Lobanov, H. Guo, M. L. Gorodetsky, and T. J. Kippenberg, Physical Review Letters **122**, 013902 (2019).
[30] T. Herr, V. Brasch, J. D. Jost, I. Mirgorodskiy, G. Lihachev, M. L. Gorodetsky, and T. J. Kippenberg, Physical Review Letters **113**, 123901 (2014).
[31] Q.-F. Yang, X. Yi, K. Y. Yang, and K. Vahala, Optica **3**, 1132 (2016).
[32] See Supplemental Material for details, which also includes Refs. [22,23,26,27,29,33,45].
[33] H. Guo, M. Karpov, E. Lucas, A. Kordts, M. Pfeiffer, V. Brasch, G. Lihachev, V. Lobanov, M. Gorodetsky, and T. Kippenberg, Nature Physics **13**, 94 (2017).
[34] Y. Wang, F. Leo, J. Fatome, M. Erkintalo, S. G. Murdoch, and S. Coen, Optica **4**, 855 (2017).
[35] P. Parra-Rivas, D. Gomila, P. Colet, and L. Gelens, The European Physical Journal D **71**, 198 (2017).
[36] A. G. Vladimirov, S. V. Gurevich, and M. Tlidi, Physical Review A **97**, 013816 (2018).
[37] H. Taheri, A. B. Matsko, and L. Maleki, The European Physical Journal D **71**, 153 (2017).
[38] I. Coddington, N. Newbury, and W. Swann, Optica **3**, 414 (2016).
[39] C. Milián, Y. V. Kartashov, D. V. Skryabin, and L. Torner, Physical review letters **121**, 103903 (2018).
[40] A. Dutt, C. Joshi, X. Ji, J. Cardenas, Y. Okawachi, K. Luke, A. L. Gaeta, and M. Lipson, Science advances **4**, e1701858 (2018).
[41] M.-G. Suh, Q.-F. Yang, K. Y. Yang, X. Yi, and K. J. Vahala, Science **354**, 600 (2016).
[42] M.-G. Suh and K. J. Vahala, Science **359**, 884 (2018).
[43] P. Trocha, M. Karpov, D. Ganin, M. H. Pfeiffer, A. Kordts, S. Wolf, J. Krockenberger, P. Marin-Palomo, C. Weimann, S. Randel, *et al.*, Science **359**, 887 (2018).
[44] Q.-F. Yang, B. Shen, H. Wang, M. Tran, Z. Zhang, K. Y. Yang, L. Wu, C. Bao, J. Bowers, A. Yariv, *et al.*, Science **363**, 965 (2019).
[45] L. A. Lugiato and R. Lefever, Physical Review Letters **58**, 2209 (1987).
[46] See https://doi.org/10.5281/zenodo.3560069.